ACS Catalysis

pubs.acs.org/acscatalysis

Research Article

# Photocatalytic Methylation of Nonactivated $sp^3$ and $sp^2$ C−H Bonds Using Methanol on GaN

Mingxin Liu,[‖] Zihang Qiu,[‖] Lida Tan,[‖] Roksana T. Rashid, Sheng Chu, Yunen Cen, Ziling Luo, Rustam Z. Khaliullin, Zetian Mi,* and Chao-Jun Li*

Cite This: *ACS Catal.* 2020, 10, 6248−6253

Read Online

ACCESS | Metrics & More | Article Recommendations | Supporting Information

**ABSTRACT:** Although the development of C−H functionalization methods has enlightened many reactivities in chemistry, the direct functionalization of unactivated C−H bonds, which are particularly common in petroleum compounds, is still faced with great difficulty. Herein, we describe a photocatalytic approach that allows direct methylation of unactivated $sp^3$ and $sp^2$ C−H bonds using methanol as the methylation reagent, with gallium nitride as a powerful yet robust catalyst. Mechanistic studies suggested that the methanol is dehydrated into methyl carbene intermediate via a bimolecular mechanism.

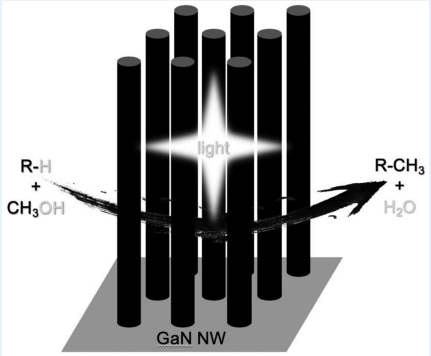


**KEYWORDS:** *methylation, photocatalysis, methanol, GaN, semiconductor*



The development of a novel C−H functionalization strategy has been enabling powerful tools for chemical conversions,[1−3] unlocking unprecedented synthetic routes for more efficient chemical production and less waste emission. However, to functionalize the unactivated C−H bonds, which are ubiquitous among the petroleum reservoir,[4,5] harsh conditions and stoichiometric reagents[6−18] are still extensively applied, generating large amounts of waste and persistent metal footprints. Recently in 2019, Antonietti and König reported the photocatalytic C−H functionalization of arenes using mesoporous graphitic carbon nitride,[19] which achieved broad functional tolerance. On the other hand, DMSO is still required as the solvent, which is not easy to separate and reuse.[20] In addition, simple arenes and alkanes are not reactive. Efficient functionalization of unactivated C−H bonds with environmentally benign reagents, mild reaction procedures, and enhanced reliability still poses a fundamental challenge.

Praised by many elegant studies,[21] methanol, being easily accessible from $CO_2$ reduction, is considered one of the most promising sustainable resources for the future. In 2017, our group has demonstrated the use of methanol for photochemical C−H methylation of heteroarenes,[22] which is crucial in biochemistry and pharmaceutical science.[23−30] However, as such activation generates a nucleophilic hydroxymethyl radical, electrophilic starting materials are mandatory which thus limits the substrate scope to only N-heterocyclic aromatics. The key to overcome this limitation is the development of alternative methanol activation that could overcome the high bond strength of the methanol C−O bond and removes the nucleophilic oxygen. Early in 2019, a preliminary discovery from our group showed that methanol can be photocatalytically activated into methyl carbene ($:CH_2$) on the surface of the gallium nitride nanowire (GaN NW).[31] We then postulated the possibility to utilize this key carbene intermediate to achieve C−H methylation of more general unactivated C−H bonds. Herein, we present such photodriven C−H methylation using methanol at ambient conditions on GaN NW catalyst.

The GaN NW was grown via plasma-assisted molecular beam epitaxy (PA-MBE, see Figure S1 in the Supporting Information). n- and p-type dopings ($Si^{4+}$, $Mg^{2+}$, respectively) were applied to grow the corresponding n-GaN NW and p-GaN NWs (the standard effusion cell temperatures of Si and Mg are 1350 and 265 °C, respectively), as significant near-surface energy band bending can be observed with doping. The undoped GaN NW was also grown and will be referred to as intrinsic *i*-GaN NW. The surface area of the GaN NW can be calculated from the density, length, and diameter of the NW. The typical growth time for the NWs is 4 h, yielding a surface area of the top plane (polar c-plane) and of the side plane

Received: February 21, 2020
Revised: May 5, 2020
Published: May 6, 2020

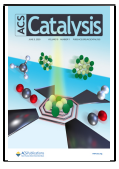

(nonpolar m-plane) of 0.17 and 5.53 $m^2\ g^{-1}$, respectively. The p-GaN NW grown for 2 h was also used in this study, showing a c-plane area of 0.17 $m^2\ g^{-1}$ and an m-plane area of 2.77 $m^2\ g^{-1}$.

We then chose to study the methylation of benzene (**1a**) into toluene (**2a**) first. A 3.5 $cm^2$ slice of a GaN NW grown for 4 h (equal to 0.35 mg GaN) was then placed at the bottom of a 120 mL glass flange equipped with a sealing O-ring and an evacuation seal. The flange was capped with a quartz window and evacuated using a vacuum oil pump until the internal pressure dropped below $5 \times 10^{-2}$ mbar. 5 $\mu$L (equal to 0.124 mmol) of HPLC grade methanol and 10 $\mu$L (equal to 0.112 mmol) of HPLC grade **1a** were then introduced through the seal into the flange before the flange was cooled to 4 °C in a chiller and irradiated with a 300 W full-arc xenon lamp for 12 h (see Figure S2 in the Supporting Information). The gas phase inside the flange was analyzed using a valve syringe and gas chromatography mass spectrometer (GC-MS). To our delight, by using the p-doped GaN NW, 0.038 mmol of **2a** was detected, which corresponds to a 34% yield (Figure 1A). This

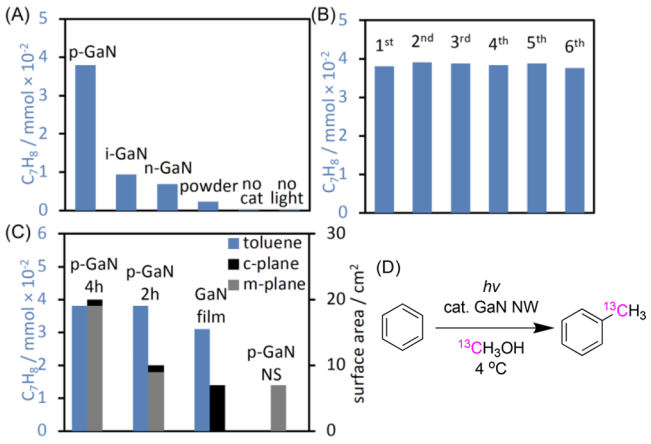


**Figure 1.** Catalyst performance examination. Reaction conditions: 10 $\mu$L of benzene and 5 $\mu$L of methanol were injected into an evacuated flange reactor containing a slice of p-GaN NW (grown for 2 h). The reactor was then chilled at 4 °C and illuminated by a Xe lamp for 12 h. (A) Performance of catalyst with different dopings. (B) Catalyst recyclability test. (C) Catalysts performance with quantification of surface area. (D) Isotope labeling experiment.

yield is much higher than the methanol-to-ethanol conversion that we published earlier under similar reaction conditions.[27] Further methylation of **2a** was also identified on the GC-MS, but the regioselectivity was unable to be determined due to the extremely low yield. In addition, no ethanol was detected in the reaction, indicating that the methyl carbene intermediate generated from methanol prefers to attack the **1a**'s $sp^2$ C−H bond rather than the methanol's $sp^3$ C−H bond. We then examined the **1a**-to-**2a** conversion using the n-GaN NW, which dramatically reduced the **2a** yield to 0.0069 mmol. *i*-GaN also gave a reduced yield of 0.0094 mmol. These results demonstrated the importance of a downward near-surface band bending granted by the p-GaN, giving an electron-enriched surface.[31] Using 0.35 mg of commercial GaN powder, the reaction gave 0.0023 mmol of **2a** while no **2a** was detected in the absence of either GaN or light. To examine the robustness of the catalyst, six consecutive methylation experiments were conducted by recycling the same catalyst; the catalyst showed no decrease in activity (Figure 1B). A 3.5 $cm^2$ slice of a p-GaN NW grown for 2 h instead of 4 h (equal to 0.17 mg of GaN) was also examined for catalytic **1a**-to-**2a** conversion, and it gave a similar 0.038 mmol yield of **2a**, resulting in a catalytic efficiency of 18 100 $\mu$mol $g_{cat}^{-1}\ h^{-1}$ (Figure 1C). Considering the similar yields granted by p-GaN grown for 2 and 4 h, which possess identical c-plane areas but different m-plane areas, p-GaN thin film was then examined under the same reaction conditions in order to determine the surface being responsible for the **1a**-to-**2a** conversion. The experiment gave 0.031 mmol of **2a**. We also synthesized a p-GaN nanosheet (NS) with no c-plane as the catalyst,[32] which gave no desired **1a**-to-**2a** conversion, to further support the hypothesis that the c-plane is solely responsible for the **1a**-to-**2a** conversion. This phenomenon is consistent with our previous study which indicates the methanol to carbene conversion being achieved solely on the c-plane.[31] The isotope labeling experiment using $^{13}CH_3OH$ also gave $^{13}C$ labeled **2a** (Figure 1D; see also Figure S6 for characterization).

Encouraged by the efficiency of the photocatalytic conversion in the gas phase **1a**-to-**2a** reaction, we then embarked on the optimization of the reported method for more synthetic utilization (Table 1). For the methylation of

**Table 1. Reaction Condition Optimization**

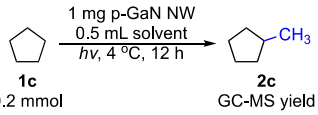


| entry[a] | solvent | additive | yield |
|---|---|---|---|
| 1[b] | N/A | 1 equiv $CH_3OH$ | < 1% |
| 2 | N/A | 1 equiv $CH_3OH$ | 11% |
| 3 | $CH_3OH$ | N/A | 7% |
| 4 | $CH_2Cl_2$ | 1 equiv $CH_3OH$ | 2% |
| 5 | $H_2O$ | 1 equiv $CH_3OH$ | < 1% |
| 6 | $CH_3CN$ | 1 equiv $CH_3OH$ | 21% |
| 7 | $CH_3CN$ | N/A | 21% |
| 8 | $CH_3OH$ | 0.2 equiv TFA | 16% |
| 9 | $CH_3OH$ | 0.2 equiv HCl | 8% |
| 10 | $CH_3OH$ | 0.2 equiv AcOH | 7% |
| 11 | $CH_3OH$ | 2 equiv TFA | 22% |
| 12[c] | $CH_3OH$ | 2 equiv TFA | 29% |
| 13[d] | $CH_3OH$ | 2 equiv TFA | 20% |
| 14[e] | $CH_3OH$ | 2 equiv TFA | 19% |
| 15[f] | $CH_3OH$ | 2 equiv TFA | 17% |
| 16[c] | N/A | 2 equiv TFA | N.D. |

[a]Reaction conditions: all reagents were injected into an evacuated flange reactor containing a slice of p-GaN NW (grown for 2 h). The reactor was then chilled at 4 °C and illuminated by a Xe lamp for 12 h. [b]The reaction uses 0.17 mg catalyst loading. [c]The catalyst was deposited with 5 wt % Cu NP. [d]The catalyst was deposited with 5 wt % Fe NP. [e]The catalyst was deposited with 5 wt % Ag NP. [f]The catalyst was deposited with 5 wt % Au NP.

the $sp^3$ substrate, cyclopentane (**1c**), only less than 1% yield of methylcyclopentane (**2c**) was obtained (Table 1, entry 1). Using this conversion as the model reaction for optimization, we first increased the catalyst (p-GaN NW, 2 h growth time) loading from 0.17 to 1 mg and obtained an 11% **2c** yield (Table 1, entry 2). Next, we examined the addition of solvent inside the reactor flange to convert the previous gas-phase reaction into a more synthetically useful solvent reaction. Various solvents, such as methanol (Table 1, entry 3), dichloromethane (Table 1, entry 4), water (Table 1, entry 5), and acetonitrile (Table 1, entry 6), were examined. Surprisingly, acetonitrile gave the highest yield of 21%.


https://dx.doi.org/10.1021/acscatal.0c00881
ACS Catal. 2020, 10, 6248−6253

**Table 2. Substrate Scope Investigation**

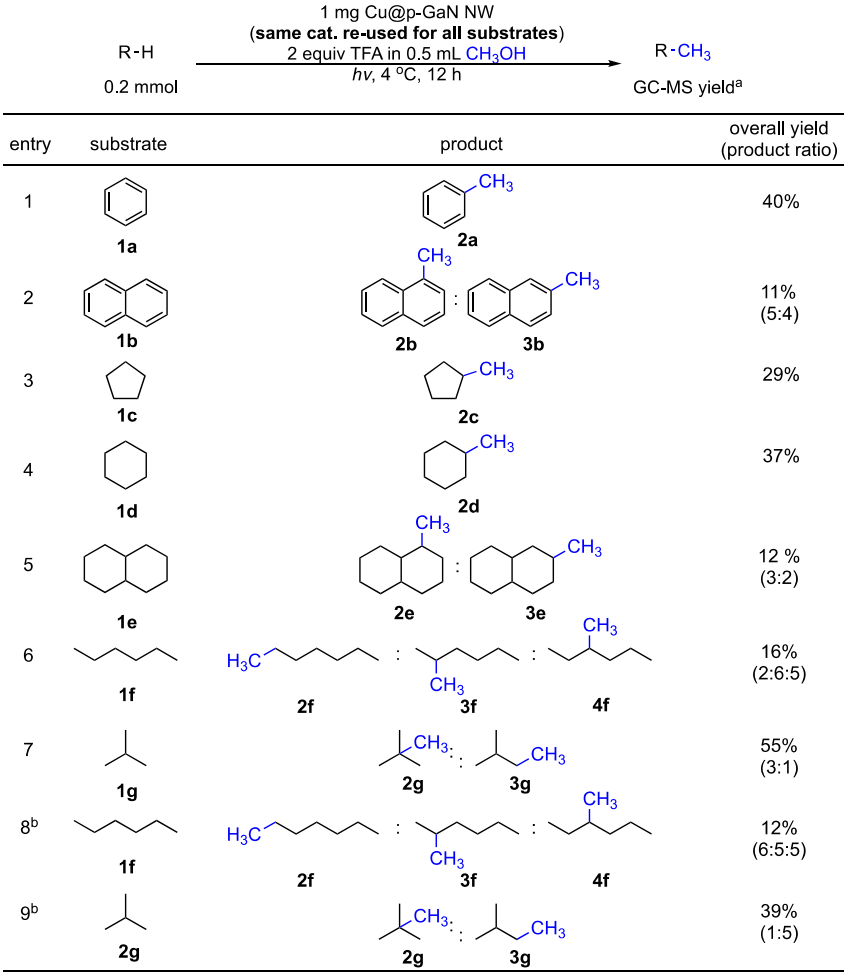


[a]Reaction conditions: 0.2 mmol of alkane, 0.4 TFA, and 0.5 mL of methanol were injected into an evacuated flange reactor containing a slice of p-GaN NW (grown for 2 h). The reactor was then chilled at 4 °C and illuminated by a Xe lamp for 12 h. [b]Reaction was conducted at 90 °C.

However, when the control reaction was conducted using acetonitrile as the sole solvent without methanol (Table 1, entry 7), a similar yield of 21% was still obtained. This indicates that acetonitrile is consumed as the reactant and serves as a better methyl donor than methanol, possibly due to the −CN group being a better leaving group than −OH. Inspired by this, we reasoned that the introduction of acid in the reaction mixture may boost the reactivity by making −OH a better leaving group. We started by adding 0.2 equiv of trifluoroacetic acid (TFA) into the reaction mixture using methanol as the solvent (Table 1, entry 8), giving 16% yield of **2c**. Other acids such as HCl (Table 1, entry 9) and acetic acid (Table 1, entry 10) did not grant increased reactivity. We then raised the loading of TFA, and the highest yield was granted with 2 equiv (Table 1, entry 11) TFA loading, giving 22% yield. Finally, as copper is known to facilitate the C−H insertion of methyl carbene,[33] a p-GaN NW deposited with a copper nanoparticle (Cu NP, see Figure S13 for characterization) was used as the catalyst and granted a 29% yield of **2c** (Table 1, entry 12). The deposition of other metals, such as iron (Table 1, entry 13), silver (Table 1, entry 14), and gold (Table 1, entry 15), did not increase the reactivity. The control experiment also showed that the reaction did not proceed without methanol (Table 1, entry 16).

We then began to investigate the reaction scope by using the same catalyst over-and-over for all substrates (Table 2). Compared to **1a**, which was methylated to **2a** with 40% yield (Table 2, entry 1), naphthalene (**1b**) gave an overall 11% yield of methylnaphthalene, with a slight selectivity for 1-methylnaphthalene (**2b**) instead of 2-methylnaphthalene (**3b**) (Table 2, entry 2). For $sp^3$ substrates, **1c** gave 29% methylation yield of **2c** (Table 2, entry 3). Cyclohexane (**1d**) was examined to give an increased methylcyclohexane (**2d**) yield of 37% (Table 2, entry 4). The increase of efficiency might be due to the affinity of the six-member ring with the wurtzite crystal structure of GaN, as well as the change in the ring strain and the increased $sp^2$ character in the molecular orbital.[34] *trans*-Decalin (**1e**) gave a 3:2 ratio of 1-methyldecalin (**2e**) and 2-methyldecalin (**3e**), with an overall 12% yield (Table 2, entry 5). We then examined the methylation of *n*-hexane (**1f**), which could give three methylation products depending on the regioselectivity of the methylation. Astonishingly, the ratio of the generated 1-,2-,3-methylated hexane (*n*-heptane, **2f**; 2-methylhexane, **3f**; 3-methylhexane, **4f**) was observed to be 2:6:5 with an overall yield of 16% (Table 2, entry 6). Similarly, the methylation of isobutane (**1g**) also disfavors 1° C−H, giving a 3:1 ratio of neopentane (**2g**) and 2-methylbutane (**3g**) with an increased overall yield of 55% (Table 2, entry 7). This selectivity is not consistent with classic


https://dx.doi.org/10.1021/acscatal.0c00881
ACS Catal. 2020, 10, 6248−6253

knowledge of free-carbenes[35,36] and therefore implies a strong interference of the GaN surface on the behavior of the photogenerated methyl carbene. To test this hypothesis, the reaction temperature was raised to 90 °C to promote the desorption of the carbene on the GaN surface. It was observed that the methylation of both **1f** and **1g** gave increased selectivity for 1° C−Hs (Table 2, entries 8 and 9), which is more consistent with classic carbene chemistry. This suggests a strong tendency for the generated carbenes to be adsorbed on the GaN surface. It should be noted that the GaN NW catalyst shows no significant sign of degradation after nine consecutive catalytic cycles (see Figure S13 in the Supporting Information).

As indicated by our previous study,[31] the reaction began with the dehydration of methanol molecules into methyl carbenes on the surface of p-GaN under the irradiation of the Xe lamp. To further examine this mechanism, we periodically monitored the generation of toluene under the optimized reaction conditions over the first 2 h (Figure 2A). Then, the

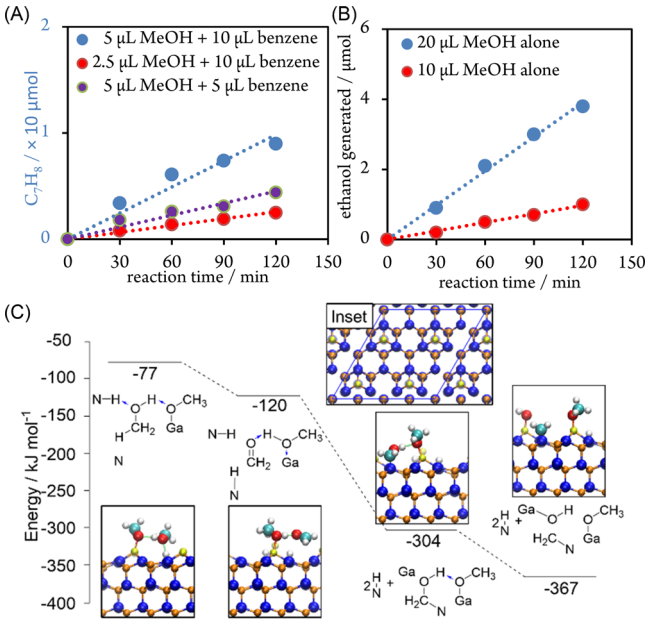


**Figure 2.** Reaction kinetic studies and the proposed mechanism. (A) Kinetic study of benzene-to-toluene conversion. (B) Kinetic study of methanol-to-ethanol conversion. (C) Proposed mechanism of the carbene formation with the PBE/DZVP energy profile. The inset shows the model of the nitrogen terminated c-plane of GaN with one Ga adatom in an H3 site of a 2-by-2 surface unit cell. Blue, red, cyan, gray, and yellow spheres denote positions of nitrogen, oxygen, carbon, and hydrogen atoms, respectively. Gallium adatoms are shown in yellow while other gallium atoms are shown in orange.

initial methanol loading was reduced by half (2.5 $\mu$L), and it was found that the reaction rate was significantly reduced to approximately 1/4 compared to the optimized reaction. As a benchmark, we also decreased the benzene amount (to 5 $\mu$L), and the reaction rate was reduced to approximately 1/2. This indicates that the reaction rate equation is likely to be proportional to the benzene activity coefficient and the methanol activity coefficient squared, suggesting a mechanism involving two methanol molecules. A similar test was also conducted for our previous methanol-to-ethanol conversion and gave a similar reaction rate decrease to 1/4 of the optimized yield when the methanol loading was halved (Figure 2B). Therefore, the rate-determining step in the initial carbene formation from methanol is likely to involve two methanol molecules.

Density functional theory (DFT) calculations were carried out in order to gain insight into elementary steps of the plausible mechanism of the two-molecule process of carbene generation and structural transformations along the pathway. All calculations were performed using the DFT module of the CP2K software package.[37] In the dual Gaussian and plane-wave scheme implemented in CP2K,[38] a double-$\zeta$ Gaussian basis set with one set of polarization functions (DZVP)[39] was used to represent spin-unrestricted orbitals. A plane-wave cutoff of 1200 Ry was used to represent the electron density. Separable norm-conserving Goedecker−Teter−Hutter pseudopotentials were used to describe the interactions between the valence electrons and ionic cores,[40,41] and the Brillouin zone was sampled at the $\Gamma$ point. The Perdew−Burke−Ernzerhof generalized gradient approximation[42] corrected to account for dispersion interactions[43] was used as the exchange-correlation functional. The size of a simulation box along the perpendicular direction to the surface was set to 32 Å to ensure decoupling of slab periodic images. A dipole correction[44] was applied to cancel the spurious electric field in the direction perpendicular to the surface. The positions of all atoms were fully relaxed in calculations.

An atomistic model of the nitrogen terminated c-plane of GaN—often labeled as −c-plane or $(000\bar{1})$—was created following previous experimental and computational studies, which indicate that a 2 × 2 surface unit cell with one Ga adatom in an H3 site (Figure 2C) is the most stable surface reconstruction under N-rich conditions.[45,46] The slab with the surface of 4 × 4 surface unit cells containing four Ga adatoms and the depth of three cells was built to represent the NW surface (Figure 2C, inset). The opposite inactive gallium terminated +c-plane of the slab was passivated with nitrogen adatoms located in H3 sites directly under Ga adatoms.[45,46] The spin-unrestricted DFT calculations result in no unpaired electrons in the slab and thus confirm that the model satisfies the electron counting rule, indicative of surface stability.[45] The methanol dimer configuration with the lowest energy is shown as the leftmost structure in Figure 2C. It is hypothesized that the first photoinduced step of the reaction, the mechanism of which is not modeled directly here, is the migration of a hydrogen atom of the methyl group closest to an exposed nitrogen atom on the surface. The subsequent ground state surface-mediated relaxation of the $CH_2OH$ molecule results in the migration of the hydrogen atom of the hydroxyl group to a nearby Ga-bound methoxy group with the formation of a formaldehyde molecule, which quickly reorients to form a N−C bond with another surface nitrogen atom (Figure 2C). This transformation of a methanol molecule into the N-bound $CH_2OH$ intermediate is accompanied by the energy lowering of 227 kJ/mol, indicating that, despite possible missing excited-state intermediates, this final structure is thermodynamically plausible. What is important is that a nearby methoxy group plays an important role in the transformation. It participates in shuttling the hydrogen atom and serving as a surface anchor during the reorientation of the $CH_2O$ group, which explains the observed second order of the reaction in methanol. In the next step, the cleavage of the C−O is thermodynamically driven by the further energy lowering and can be facilitated by nearby protons through the formation of a $H_2O−CH_2$


https://dx.doi.org/10.1021/acscatal.0c00881
ACS Catal. 2020, 10, 6248−6253

intermediate. It is also worth noting that the generated carbene is adsorbed to the nitrogen atom of the GaN surface.

In conclusion, we have demonstrated that, by using GaN as a robust catalyst, methylations of simple alkanes and arenes using methanol can be achieved with high efficiency. In addition, it can be suggested by our experimental results that the photocatalytic methanol transformation into methyl carbene involves two methanol molecules to facilitate the elimination. Further applications regarding GaN-catalyzed hydrocarbon conversions are already underway in our lab.

## ■ ASSOCIATED CONTENT

### Supporting Information

The Supporting Information is available free of charge at https://pubs.acs.org/doi/10.1021/acscatal.0c00881.

Materials and methods and additional data and figures including an SEM image, reaction setup, chromatography results, mass spectra, TEM images, XPS spectra, and a UV−vis absorption spectrum (PDF)

## ■ AUTHOR INFORMATION


### Corresponding Authors

**Zetian Mi** − *Department of Electrical Engineering and Computer Science, University of Michigan, Ann Arbor, Michigan 48109, United States; Department of Electrical and Computer Engineering, McGill University, Montreal, Quebec H3A 0E9, Canada;* orcid.org/0000-0001-9494-7390; Email: ztmi@umich.edu

**Chao-Jun Li** − *Department of Chemistry and FRQNT Centre for Green Chemistry and Catalysis, McGill University, Montreal, Quebec H3A 0B8, Canada;* orcid.org/0000-0002-3859-8824; Email: cj.li@mcgill.ca

### Authors

**Mingxin Liu** − *Department of Chemistry and FRQNT Centre for Green Chemistry and Catalysis, McGill University, Montreal, Quebec H3A 0B8, Canada; Department of Electrical Engineering and Computer Science, University of Michigan, Ann Arbor, Michigan 48109, United States*

**Zihang Qiu** − *Department of Chemistry and FRQNT Centre for Green Chemistry and Catalysis, McGill University, Montreal, Quebec H3A 0B8, Canada;* orcid.org/0000-0002-8628-6497

**Lida Tan** − *Department of Chemistry and FRQNT Centre for Green Chemistry and Catalysis, McGill University, Montreal, Quebec H3A 0B8, Canada*

**Roksana T. Rashid** − *Department of Electrical and Computer Engineering, McGill University, Montreal, Quebec H3A 0E9, Canada*

**Sheng Chu** − *Department of Electrical and Computer Engineering, McGill University, Montreal, Quebec H3A 0E9, Canada;* orcid.org/0000-0001-9850-5012

**Yunen Cen** − *Department of Chemistry and FRQNT Centre for Green Chemistry and Catalysis, McGill University, Montreal, Quebec H3A 0B8, Canada*

**Ziling Luo** − *Department of Chemistry and FRQNT Centre for Green Chemistry and Catalysis, McGill University, Montreal, Quebec H3A 0B8, Canada*

**Rustam Z. Khaliullin** − *Department of Chemistry and FRQNT Centre for Green Chemistry and Catalysis, McGill University, Montreal, Quebec H3A 0B8, Canada;* orcid.org/0000-0002-9073-6753

Complete contact information is available at: https://pubs.acs.org/10.1021/acscatal.0c00881

### Author Contributions

‖M.L., Z.Q, and L.T. contributed equally.


### Notes

The authors declare no competing financial interest.

## ■ ACKNOWLEDGMENTS

We are grateful for the support of the following funding agencies: Canada Research Chair (Tier 1) foundation Natural Science and Engineering Research Council of Canada Fonds de recherche du Quebec—Nature et Technologies Canada Foundation for Innovation Emission Reduction Alberta.

## ■ REFERENCES


(1) Periana, R. A.; Bhalla, G.; Tenn, W. J.; Young, K. J. H.; Liu, X. Y.; Mironov, O.; Jones, C.; Ziatdinov, V. R. Perspectives on some Challenges and Approaches for Developing the Next Generation of Selective, Low Temperature, Oxidation Catalysts for Alkane Hydroxylation Based on the CH Activation Reaction. *J. Mol. Catal. A: Chem.* **2004**, *220*, 7−25.

(2) Li, X.; Ouyang, W.; Nie, J.; Ji, S.; Chen, Q.; Huo, Y. Recent Development on Cp*Ir(III)-Catalyzed C−H Bond Functionalization. *ChemCatChem* **2020**, *12*, 2358.

(3) He, J.; Wasa, M.; Chan, K. S. L.; Shao, Q.; Yu, J.-Q. Palladium-Catalyzed Transformations of Alkyl C−H Bonds. *Chem. Rev.* **2017**, *117*, 8754−8766.

(4) Edenhofer, O., Pichs-Madruga, R., Sokona, Y., Farahani, E., Kadner, S., Seyboth, K., Adler, A., Baum, I., Brunner, S., Eickemeier, P., Kriemann, B., Savolainen, J., Schlömer, S., von Stechow, C., Zwickel, T., Minx, J. C., Eds. *Intergovernmental Panel on Climate Change, 2014: Climate Change 2014: Mitigation of Climate Change*; Cambridge University Press: Cambridge, 2014.

(5) Tullo, A. H. Why the Future of Oil is in Chemicals, not Fuels. *Chem. Eng. News* **2019**, *97* (8), 48−53.

(6) Snieckus, V. Directed Ortho Metalation. Tertiary Amide and O-carbamate Directors in Synthetic Strategies for Polysubstituted Aromatics. *Chem. Rev.* **1990**, *90*, 879−933.

(7) Barsky, L.; Gschwend, H. W.; McKenna, J.; Rodriguez, H. R. Ortho-lithiation. A Regiospecific Route to Ortho-substituted Aryl Ketones. *J. Org. Chem.* **1976**, *41*, 3651−3652.

(8) Townsend, C. A.; Bloom, L. M. Studies of Methoxymethyl-directed Metalation. *Tetrahedron Lett.* **1981**, *22*, 3923−3924.

(9) Chen, X.; Li, J.-J.; Hao, X.-S.; Goodhue, C. E.; Yu, J.-Q. Palladium-Catalyzed Alkylation of Aryl C−H Bonds with $sp^3$ Organotin Reagents Using Benzoquinone as a Crucial Promoter. *J. Am. Chem. Soc.* **2006**, *128*, 78−79.

(10) Zhang, Y.; Feng, J.; Li, C.-J. Palladium-Catalyzed Methylation of Aryl C−H Bond by Using Peroxides. *J. Am. Chem. Soc.* **2008**, *130*, 2900−2901.

(11) Romero-Revilla, J. A.; García-Rubia, A.; Goméz Arrayás, R.; Fernández-Ibáñez, M. Á.; Carretero, J. C. Palladium-Catalyzed Coupling of Arene C−H Bonds with Methyl- and Arylboron Reagents Assisted by the Removable 2-Pyridylsulfinyl Group. *J. Org. Chem.* **2011**, *76*, 9525−9530.

(12) Giri, R.; Maugel, N.; Li, J.-J.; Wang, D.-H.; Breazzano, S. P.; Saunders, L. B.; Yu, J.-Q. Palladium-Catalyzed Methylation and Arylation of $sp^2$ and $sp^3$ C−H Bonds in Simple Carboxylic Acids. *J. Am. Chem. Soc.* **2007**, *129*, 3510−3511.

(13) Chen, Q.; Ilies, L.; Yoshikai, N.; Nakamura, E. Cobalt-Catalyzed Coupling of Alkyl Grignard Reagent with Benzamide and 2-Phenylpyridine Derivatives through Directed C−H Bond Activation under Air. *Org. Lett.* **2011**, *13*, 3232−3234.

(14) Shang, R.; Ilies, L.; Nakamura, E. Iron-Catalyzed Directed $C(sp^2)$−H and $C(sp^3)$−H Functionalization with Trimethylaluminum. *J. Am. Chem. Soc.* **2015**, *137*, 7660−7663.

(15) Pan, F.; Lei, Z.-Q.; Wang, H.; Li, H.; Sun, J.; Shi, Z.-J. Rhodium(I)-Catalyzed Redox-Economic Cross-Coupling of Carboxylic Acids with Arenes Directed by N-Containing Groups. *Angew. Chem., Int. Ed.* **2013**, *52*, 2063−2067.
(16) Hu, L.; Liu, X.; Liao, X. Nickel-Catalyzed Methylation of Aryl Halides with Deuterated Methyl Iodide. *Angew. Chem., Int. Ed.* **2016**, *55*, 9743−9747.
(17) Neufeldt, S. R.; Seigerman, C. K.; Sanford, M. S. Mild Palladium-Catalyzed C−H Alkylation Using Potassium Alkyltrifluoroborates in Combination with $MnF_3$. *Org. Lett.* **2013**, *15*, 2302−2305.
(18) Yao, B.; Song, R.-J.; Liu, Y.; Xie, Y.-X.; Li, J.-H.; Wang, M.-K.; Tang, R.-Y.; Zhang, X.-G.; Deng, C.-L. Palladium-Catalyzed C-H Oxidation of Isoquinoline N-Oxides: Selective Alkylation with Dialkyl Sulfoxides and Halogenation with Dihalo Sulfoxides. *Adv. Synth. Catal.* **2012**, *354*, 1890−1896.
(19) Ghosh, I.; Khamrai, J.; Savateev, A.; Shlapakov, N.; Antonietti, M.; König, B. Organic Semiconductor Photocatalyst Can Bifunctionalize Arenes and Heteroarenes. *Science* **2019**, *365*, 360−366.
(20) Roy, K.-M. Sulfones and Sulfoxides. In *Ullmann's Encyclopedia of Industrial Chemistry*; Wiley-VCH: Weinheim, 2002.
(21) Tian, P.; Wei, Y.; Ye, M.; Liu, Z. Methanol to Olefins (MTO): From Fundamentals to Commercialization. *ACS Catal.* **2015**, *5*, 1922−1938.
(22) Liu, W.; Yang, X.; Zhou, Z.-Z.; Li, C.-J. Simple and Clean Photo-Induced Methylation of Heteroarenes with MeOH. *Chem.* **2017**, *2*, 688−702.
(23) Barreiro, E. J.; Kümmerle, A. E.; Fraga, C. A. M. The Methylation Effect in Medicinal Chemistry. *Chem. Rev.* **2011**, *111*, 5215−5246.
(24) Schönherr, H.; Cernak, T. Profound Methyl Effects in Drug Discovery and a Call for New C-H Methylation Reactions. *Angew. Chem., Int. Ed.* **2013**, *52*, 12256−12267.
(25) Angell, R.; Aston, N. M.; Bamborough, P.; Buckton, J. B.; Cockerill, S.; deBoeck, S. J.; Edward, C. D.; Holmes, D. S.; Jones, K. L.; Laine, D. I.; Patel, S.; Smee, P. A.; Smith, K. J.; Somers, D. O.; Walker, A. L. Biphenyl Amide p38 Kinase Inhibitors 3: Improvement of Cellular and *in vivo* Activity. *Bioorg. Med. Chem. Lett.* **2008**, *18*, 4428−4432.
(26) Nan, X.; Ng, H.-H.; Johnson, C. A.; Laherty, C. D.; Turner, B. M.; Eisenman, R. N.; Bird, A. Transcriptional Repression by the Methyl-CpG-binding Protein MeCP2 Involves a Histone Deacetylase Complex. *Nature* **1998**, *393*, 386−389.
(27) Lachner, M.; O'Carroll, D.; Rea, S.; Mechtler, K.; Jenuwein, T. Methylation of Histone H3 Lysine 9 Creates a Binding Site for HP1 Proteins. *Nature* **2001**, *410*, 116−120.
(28) Jaenisch, R.; Bird, A. Epigenetic Regulation of Gene Expression: How the Genome Integrates Intrinsic and Environmental Signals. *Nat. Genet.* **2003**, *33*, 245−254.
(29) Okano, M.; Bell, D. W.; Haber, D. A.; Li, E. DNA Methyltransferases Dnmt3a and Dnmt3b are Essential for *de novo* Methylation and Mammalian Development. *Cell* **1999**, *99*, 247−257.
(30) Choy, J. S.; Wei, S.; Lee, J. Y.; Tan, S.; Chu, S.; Lee, T.-H. DNA Methylation Increases Nucleosome Compaction and Rigidity. *J. Am. Chem. Soc.* **2010**, *132*, 1782−1783.
(31) Liu, M.; Wang, Y.; Kong, X.; Rashid, R. T.; Chu, S.; Li, C.-C.; Hearne, Z.; Guo, H.; Mi, Z.; Li, C.-J. Direct Catalytic Methanol-to-Ethanol Photo-conversion via Methyl Carbene. *Chem.* **2019**, *5*, 858−867.
(32) Chowdhury, F. A.; Trudeau, M. L.; Guo, H.; Mi, Z. A Photochemical Diode Artificial Photosynthesis System for Unassisted High Efficiency Overall Pure Water Splitting. *Nat. Commun.* **2018**, *9*, 1707.
(33) Díaz-Requejo, M. M.; Belderraín, T. R.; Nicasio, M. C.; Trofimenko, S.; Pérez, P. J. Intermolecular Copper-Catalyzed Carbon−Hydrogen Bond Activation via Carbene Insertion. *J. Am. Chem. Soc.* **2002**, *124*, 896−897.
(34) Kibria, M. G.; Qiao, R.; Yang, W.; Boukahil, I.; Kong, X.; Chowdhury, F. A.; Trudeau, M. L.; Ji, W.; Guo, H.; Himpsel, F. J.; Vayssieres, L.; Mi, Z. Atomic-Scale Origin of Long-Term Stability and High Performance of p-GaN Nanowire Arrays for Photocatalytic Overall Pure Water Splitting. *Adv. Mater.* **2016**, *28*, 8388−8397.
(35) Doyle, M. P.; Duffy, R.; Ratnikov, M.; Zhou, L. Catalytic Carbene Insertion into C−H Bonds. *Chem. Rev.* **2010**, *110*, 704−724.
(36) Doyle, M. P.; Westrum, L. J.; Wolthuis, W. N. E.; See, M. M.; Boone, W. P.; Bagheri, V.; Pearson, M. M. Electronic and Steric Control in Carbon-Hydrogen Insertion Reactions of Diazoacetoacetates Catalyzed by Dirhodium(II) Carboxylates and Carboxamides. *J. Am. Chem. Soc.* **1993**, *115*, 958−964.
(37) Wong, R. K. *p-Type Doping of GaN*. Master dissertation, University of California, Berkeley, United States.
(38) Hutter, J.; Iannuzzi, M.; Schiffmann, F.; Vandevondele, J. cp2k: Atomistic Simulations of Condensed Matter Systems. *Wiley Interdiscip. Rev. Comput. Mol. Sci.* **2014**, *4*, 15−25.
(39) VandeVondele, J.; Hutter, J. Gaussian Basis Sets for Accurate Calculations on Molecular Systems in Gas and Condensed Phases. *J. Chem. Phys.* **2007**, *127*, 114105.
(40) Goedecker, S.; Teter, M. Separable Dual-space Gaussian Pseudopotentials. *Phys. Rev. B: Condens. Matter Mater. Phys.* **1996**, *54*, 1703−1710.
(41) Krack, M. Pseudopotentials for H to Kr Optimized for Gradient-corrected Exchange-correlation Functionals. *Theor. Chem. Acc.* **2005**, *114*, 145−152.
(42) Perdew, J. P.; Burke, K.; Ernzerhof, M. Generalized Gradient Approximation Made Simple. *Phys. Rev. Lett.* **1996**, *77*, 3865−3868.
(43) Grimme, S.; Antony, J.; Ehrlich, S.; Krieg, H. A Consistent and Accurate *ab initio* Parametrization of Density Functional Dispersion Correction (DFT-D) for the 94 Elements H-Pu. *J. Chem. Phys.* **2010**, *132*, 154104.
(44) Bengtsson, L. Dipole Correction for Surface Supercell Calculations. *Phys. Rev. B: Condens. Matter Mater. Phys.* **1999**, *59*, 12301−12304.
(45) Bermudez, V. M. The Fundamental Surface Science of Wurtzite Gallium Nitride. *Surf. Sci. Rep.* **2017**, *72*, 147−315.
(46) Dreyer, C. E.; Janotti, A.; van de Walle, C. G. Absolute Surface Energies of Polar and Nonpolar Planes of GaN. *Phys. Rev. B: Condens. Matter Mater. Phys.* **2014**, *89*, No. 081305.


https://dx.doi.org/10.1021/acscatal.0c00881
*ACS Catal.* 2020, 10, 6248−6253